551.57 : 621.396.9

The microwave properties of precipitation particles

By K. L. S. GUNN and T. W. R. EAST
*McGill University, Montreal**

(Communicated by J. S. Marshall; manuscript received 19 July 1954)

SUMMARY

The theory of scattering and attenuation by rain, snow and cloud is reviewed and theoretical results are presented in the form of equations, tables and graphs, so that the radar response to meteorological particles can be calculated at six wavelengths (10, 5·7, 3·2, 1·8, 1·24 and 0·9 cm) and various temperatures. Particular emphasis is placed on developments since Ryde's comprehensive paper in 1946. Published experimental results are compared with the theory.

All results computed from the theory are contained in Tables 4 and 5. The attenuation by water vapour and oxygen is given in an Appendix.

1. INTRODUCTION

In the comparatively new subject of radar-meteorology, the theoretical paper by Ryde (1946) stands out. In it he predicted the back-scatter and attenuation by meteorological phenomena, and, in almost every respect, the results obtained in experiments have confirmed the predictions. The present contribution will review the theoretical problem in the light of developments in the years that have elapsed since Ryde's work was done, and with reference to the experimental results.

Meteorological radar equipment provides information about the structure or pattern and about the quantity of precipitation. This paper will not be concerned with the structural information obtained, but will consider the scattering from a small region in which the properties of the precipitation can be taken to be uniform, and the attenuation taken along a path of propagation as a whole.

Plane electromagnetic waves travelling through air containing precipitation are scattered and absorbed by the particles of ice, snow or water. Water, with its larger dielectric constant, scatters more strongly than ice; in addition, it has a much larger dielectric loss and therefore the attenuation due to thermal dissipation is much greater for water particles than for ice particles.

Three quantities with the dimensions of area are derived for a particle in the path of a plane travelling wave. The 'back-scatter cross-section' σ is defined in such a way that σ multiplied by the incident intensity would be the total power radiated by an isotropic source which radiates the same power in the backward direction as the scatterer. The 'scattering cross-section' Q_s is such that Q_s, multiplied by the incident intensity, is the power scattered by the particle. The 'total absorption cross-section' Q_t is such that Q_t times the incident intensity is the total power taken from the incident wave.

The scattering properties of precipitation have made possible extensive use of microwave radar sets for meteorological purposes. The radar signal from precipitation is, however, not steady like that from a point target. The received power at any instant is made up of the resultant of the signals from a very large number of particles, and depends on their exact arrangement in space, which is continually changing. Marshall and Hitschfeld (1953) have shown that an instantaneous observation of received power gives very little information about the precipitation, and the signal at any given range has to be averaged until a large number of independent returns have been received. This can be arranged by using a long-persistence display or by photographic recording so that the returns from many transmitter pulses are combined.

* The research reported in this paper has been made possible through support and sponsorship extended by the Geophysics Research Directorate of the United States Air Force Cambridge Research Center.

The equation for the average received power $\overline{P_r}$ is

$$\overline{P_r} = \frac{P_t A_e h}{8\pi r^2} \sum_1 \sigma \quad . \quad . \quad . \quad . \quad (1)$$

where P_t is the transmitted power,

h is the length of the pulse in space,

r the range from which the signal is being received,

A_e the equivalent antenna aperture,

$\sum_1 \sigma$ the total back-scatter cross-section of the particles in unit volume.

The received power is proportional to h so that the sensitivity of the system can be increased by lengthening the transmitter pulse. (If this change is accompanied by a reduction in receiver bandwidth, a further improvement in signal-to-noise ratio is obtained.) However, the range resolution is correspondingly reduced. Increasing A_e, on the other hand, improves both sensitivity and angular resolution, so that the antenna is made as large as practicable.

The equivalent aperture A_e is less than the actual area of the antenna for two reasons. Firstly, not all the power coming from the primary feed falls inside the parabolic reflector, neither is the distribution of power uniform across the aperture (see, e.g., Silver (1949) § 6.4). In normal radar systems the effective aperture A' for a point target is about 65 per cent of the actual aperture. The second reason, which applies only to distributed targets, affects weather radars. Some of the radiated power goes into side-lobes and the edges of the main beam, and though all of it strikes precipitation, some of the returned power comes from directions to which the antenna is less sensitive for reception. This means that the average receiving aperture A_e for all parts of the target is less than A', the value for the central portion. An exact value for A_e is difficult to determine, but a conservative estimate is probably 0·5 × (actual area).

The fact that the target normally fills the beam at any range accounts for the inverse square law for received power versus range, in place of the usual fourth-power law for a point target such as an aircraft. Though Eq. (1) does not mention wavelength explicitly, $\sum_1 \sigma$ increases rapidly as the wavelength decreases, as discussed in Section 3.

It will be shown in Section 3 (b) that for a wavelength λ long compared with the diameter D of the particles, the approximation

$$\sigma = \frac{\pi^5 D^6}{\lambda^4} |K|^2 \quad . \quad . \quad . \quad . \quad . \quad (2)$$

can be used, where $|K|^2$ depends on the dielectric constant of the material and varies only slowly with wavelength (Section 2). From Eqs. (1) and (2) we have

$$\overline{P_r} = \frac{\pi^4 P_t A_e h}{8r^2 \lambda^4} \sum_1 D^6 |K|^2 \quad . \quad . \quad . \quad (3)$$

So far we have neglected the attenuating effect of any precipitation through which the signal may have to pass. The intensity of plane parallel radiation is reduced, in traversing distance dx through precipitation, from I_0 to I, where

$$I = I_0 \exp\left\{-\sum_1 Q_t \, dx\right\} \quad . \quad . \quad . \quad . \quad (4)$$

The summation is over all the particles in unit volume. In practical units, the attenuation per kilometre of path length is

$$\text{attenuation (db km}^{-1}) = 0{\cdot}4343 \sum_1 Q_t, \quad . \quad . \quad . \quad (5)$$

where the summation is over one cubic metre and Q_t is in cm^2. For the case of wavelength long compared to the drop diameters (Section 3 (b)), we can use an approximation for Q_t, Eq. (14), so that Eq. (5) becomes

$$\text{attenuation (db km}^{-1}) = 0{\cdot}4343 \frac{\pi^2}{\lambda} \sum_1 D^3 \, Im\,(-K)^* \quad . \quad . \quad (6)$$

$$= 0{\cdot}4343 \frac{6\pi}{\lambda} \frac{M}{\rho} Im\,(-K),$$

where M is the water content in gm m^{-3}, and ρ is the density of water in gm cm^{-3}. For radar, the radiation travels there and back, so the numerical constant should be doubled to obtain decibels per kilometre of range.

The complete equation for the average received power $\overline{P_r'}$ allowing for two-way attenuation is then

$$\overline{P_r'} = 10^{-0{\cdot}0869 \int_0^r \left(\sum_1 Q_t\right) dx} \frac{P_t A_e h}{8\pi r^2} \sum_1 \sigma \times 10^{-10} \quad . \quad . \quad (7)$$

where $\sum_1 Q_t$ and $\sum_1 \sigma$ are in cm^2 m^{-3}, A_e is in m^2, h is in m, and r is in km. The effect of atmospheric attenuation, which is not included in this expression, will be discussed in Appendix I.

2. Dielectric properties of water and ice

To calculate the scattering and attenuation of electromagnetic waves by particles in the atmosphere, one must know the values of the complex dielectric constant ϵ for the temperature and wavelengths under consideration.

The square root of ϵ is the complex refractive index m which may be written

$$m = n - j\kappa,$$

where n is the refractive index and κ the absorption coefficient of the material. In general, the scattering and attenuation are complicated functions of m (Section 3), but in the special case of wavelength long compared to diameter,

$$\text{back-scatter} \propto |K|^2 \quad . \quad . \quad . \quad \text{from (3)}$$

$$\text{attenuation} \propto Im\,(-K) \quad . \quad . \quad . \quad \text{from (6)}$$

where $K = \dfrac{m^2 - 1}{m^2 + 2}$.

For a given substance m is a function of wavelength and temperature. Saxton and Lane (1946) measured values of n and κ for water at a few wavelengths and calculated other values in the centimetric band, for temperatures from 0° to 40°C. Since then Lane and Saxton (1952) have reported additional measurements at a lower wavelength (6·2 mm) and some more accurately determined values at 1·24 and 3·2 cm. Also, they have determined values of κ for supercooled water down to − 8°C at three wavelengths. Measurements by Collie, Hasted and Ritson (1948) at 10, 3 and 1·25 cm, and Buchanan (1952) at 3·2 and 1·27 cm agree to within a few per cent with the results of Lane and Saxton.

* *Im* is used for ' imaginary part of.'

In Table 1, the variation of the refractive index of water with temperature and wavelength is shown, and the quantities $Im\,(-K)$ and $|K|^2$ have been calculated. Values for n and κ are taken from Kerr (1951) for 10 cm wavelength, and directly from Lane and Saxton (1952) for the other wavelengths.

Measurements of the quantities n and κ for ice show that in the centimetre band both n and κ are practically independent of λ. Dunsmuir and Lamb (1945) and Lamb (1946) found κ to be a very small quantity, ranging from 12×10^{-4} at 0°C, through $1{\cdot}9 \times 10^{-4}$ at − 20°C to $1{\cdot}3 \times 10^{-4}$ at − 40°C. More recent measurements by Cumming (1952) give values for κ roughly twice those of Lamb; Cumming's value at − 12°C agrees with one obtained at that temperature by the M.I.T. Dielectric Laboratory (Cumming 1952). Both Cumming, and Lamb and Turney (1949) agree on a value of $n = 1{\cdot}78$ for ice, constant over the temperature range 0 to − 20°C. The refractive index data for ice are summarized in Table 2.

TABLE 1. VARIATION OF REFRACTIVE INDEX OF WATER WITH TEMPERATURE AND WAVELENGTH

		λ (cm)			
		10	3·21	1·24	0·62
T (°C)					
20		8·88	8·14	6·15	4·44
10	n	9·02	7·80	5·45	3·94
0		8·99	7·14	4·75	3·45
− 8			6·48	4·15	3·10
20		0·63	2·09	2·86	2·59
10	κ	0·90	2·44	2·90	2·37
0		1·47	2·89	2·77	2·04
− 8				2·55	1·77
20		0·928	0·9275	0·9193	0·8926
10	$\|K\|^2$	0·9313	0·9282	0·9152	0·8726
0		0·9340	0·9300	0·9055	0·8312
− 8				0·8902	0·7921
20		0·00474	0·01883	0·0471	0·0915
10	$Im\,(-K)$	0·00688	0·0247	0·0615	0·1142
0		0·01102	0·0335	0·0807	0·1441
− 8				0·1036	0·1713

TABLE 2. VARIATION OF REFRACTIVE INDEX* OF ICE WITH TEMPERATURE (BASED ON DATA FROM CUMMING (1952))

T (°C)			
	n	1·78	At all temperatures
0		24×10^{-4}	
− 10	κ	$7{\cdot}9 \times 10^{-4}$	
− 20		$5{\cdot}5 \times 10^{-4}$	
	$\|K\|^2$	0·197	At all temperatures. This is for ice of unit density, the value to be used when D is diameter of melted ice particle, in Eq. (3). (Marshall and Gunn (1952)).
0		$9{\cdot}6 \times 10^{-4}$	
− 10	$Im\,(-K)$	$3{\cdot}2 \times 10^{-4}$	
− 20		$2{\cdot}2 \times 10^{-4}$	

* Refractive index of ice is independent of wavelength in the centimetre band.

Snow may be considered as a mixture of two dielectrics, ice and air. According to Debye (1929), one can calculate the ratio K/ρ for a mixture of two dielectrics by adding the K/ρ values for the two substances in proportion to the mass of each. Neglecting the contribution of K/ρ for air, then K/ρ for ice-air mixtures of any density is practically constant. Cumming (1952) made measurements of the dielectric constant of snow of various densities. Using his data one finds that K/ρ varies more or less uniformly from 0·46 for snow of density 0·917 g cm^{-3} to 0·50 for density 0·22 g cm^{-3}.

3. Spherical particles

(a) *Mie's theory*

A complete theory for spherical particles of any material in a non-absorbing medium was developed by Gustav Mie (1908). Mie's work has been restated by Stratton (1941), Goldstein (1946) and by Kerr (1951). Using the notation of these later workers, the cross-sections of a spherical particle are

$$\sigma = \frac{\lambda^2}{4\pi} \left| \sum_{n=1}^{\infty} (-1)^n (2n+1)(a_n - b_n) \right|^2 \quad . \quad . \quad (8)$$

$$Q_s = \frac{\lambda^2}{2\pi} \sum_{n=1}^{\infty} (2n+1)(|a_n|^2 + |b_n|^2) \quad . \quad . \quad . \quad (9)$$

and

$$Q_t = \frac{\lambda^2}{2\pi} (-Re) \sum_{n=1}^{\infty} (2n+1)(a_n + b_n)^* \quad . \quad . \quad . \quad (10)$$

where λ = wavelength in the medium,

a_n = coefficient of the nth magnetic mode,

b_n = coefficient of the nth electric mode.

The coefficients a_n and b_n are made up of Spherical Bessel functions of order n. The arguments of the functions are α and m and contain the properties of the sphere and the wavelength; $\alpha \equiv \frac{\pi D}{\lambda}$, where D is the diameter of the sphere, and m is the complex refractive index of the material discussed in Section 2.

Eqs. (9) and (10) have been computed by Lowan (1949) for water spheres at 18°C for various wavelengths between 3 mm and 10 cm.

(b) *Small spheres (Rayleigh approximation)*

By expanding the a's and b's in ascending order of α for $n = 1, 2 \ldots$, formulae for Q_s and Q_t can be obtained which apply to small values of α. Neglecting terms of higher than sixth power of α, only a_1, b_1 and b_2 are significant, and they are

$$a_1 = -\frac{j}{45}(m^2 - 1)\alpha^5 \quad . \quad . \quad . \quad . \quad . \quad . \quad (11a)$$

$$b_1 = -\frac{2j}{3}\frac{m^2 - 1}{m^2 + 2}\alpha^3 \left(1 + \frac{3}{5}\frac{m^2 - 2}{m^2 + 2}\alpha^2 - \frac{2j}{3}\frac{m^2 - 1}{m^2 + 2}\alpha^3\right) \quad . \quad (11b)$$

$$b_2 = \frac{j}{15}\frac{m^2 - 1}{2m^2 + 3}\alpha^5. \quad . \quad . \quad . \quad . \quad . \quad (11c)$$

* *Re* signifies 'real part of.'

For diameters small compared with the wavelength, we can obtain approximate formulae for σ and Q_s by putting $\alpha \ll 1$ into these equations. Then, only the leading term of b_1, the coefficient of the first electric mode, need be considered, and the contribution to σ and Q_s of all higher order terms in the a's and b's can be neglected. The resulting formulae are known as the Rayleigh approximations :

$$\sigma = \frac{\lambda^2}{2\pi} \cdot 2\alpha^6 \left|\frac{m^2-1}{m^2+2}\right|^2 = \frac{\pi^5 |K|^2}{\lambda^4} D^6 \quad . \quad . \quad . \quad (12)$$

$$Q_s = \frac{\lambda^2}{2\pi} \cdot \frac{4}{3} \alpha^6 \left|\frac{m^2-1}{m^2+2}\right|^2 . \quad . \quad . \quad . \quad . \quad (13)$$

The total absorption cross-section Q_t is given by Eq. (10) in which the real parts of the coefficients a and b have to be obtained. In this case, however, it does not always happen that the leading term in b_1 contributes the most to Q_t. Indeed, if m is purely real, the α^3 and α^5 terms of b_1 are imaginary and contribute nothing to Q_t, and of the terms listed in Eqs. (11) only the α^6 term of b_1 will appear in Q_t.

At this stage it is convenient to introduce a fourth cross-section Q_a, the absorption cross-section, to account for the power taken from the incident wave which is dissipated internally as heat and not scattered; it is simply $(Q_t - Q_s)$. Putting $\alpha \ll 1$, the contribution to Q_t of the α^6 term in b_1 is the same as the leading term in Q_s, so that this term does not appear in Q_a. Then the leading term in Q_s is given by Eq. (13) and the leading term in Q_a comes from the α^3 term in b_1 and is given by

$$Q_a = \frac{\lambda^2}{2\pi} \cdot 2\alpha^3 \, Im\left(-\frac{m^2-1}{m^2+2}\right) \text{ for } \alpha \ll 1 \quad . \quad . \quad . \quad (14)$$

and, of course,

$$Q_t = Q_a + Q_s. \quad . \quad . \quad . \quad . \quad (15)$$

For a pure ' lossless ' dielectric $Q_a = 0$ so that $Q_t = Q_s$ and is given by Eq. (13). For a very ' lossy ' dielectric like *water* and particle sizes such that $\alpha \ll 1$, $Q_s \ll Q_a$ so that $Q_t \simeq Q_a$ and is given by Eq. (14). For *ice* at 0°C and in the size range of snowflakes, at centimetre wavelengths, Q_a and Q_s are comparable and both must be calculated; Q_t is their sum.

In the various published treatments of the problem of spherical particles, a few errors have been noticed. These are discussed in Appendix II.

(c) *Larger spheres*

F. T. Haddock (1948) has computed for water at 18°C the ratio between Q_t, calculated from Lowan's (1949) Bureau of Standards tables, and Q_t, calculated from Eq. (14), assuming $Q_t = Q_a$. This ratio Q_t (Mie)/Q_t (Rayleigh) is plotted in Fig. 1 for various wavelengths. Ryde's (1946) Fig. 3 is a similar plot, but of

$$f_a = \frac{Q_t \text{ (Mie)}}{\text{geometrical cross-section}}$$

for a wavelength a little over 1 cm.

The region of α in which the exact value of Q_t given by Eq. (10) and the approximate value given by Eq. (15) [i.e. by (13) and (14)] are nearly equal we have called the ' Rayleigh region for attenuation.' The diameters of cloud particles are well inside this region for all wavelengths down to 3 mm. Rain will be discussed in Section 4.

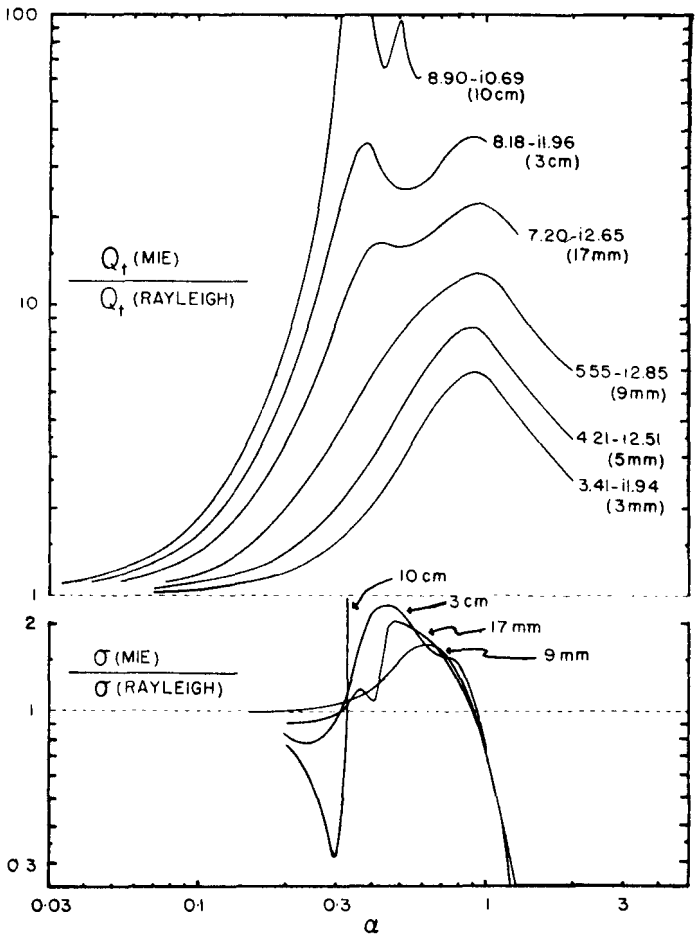

Figure 1. Ratio of actual attenuation (upper) and actual back-scattering (lower) to that given by the Rayleigh approximation, for water at 18°C. In the upper diagram the complex refractive index and wavelength (in parenthesis) are shown for each curve.

The corresponding situation for back-scatter is shown also in Fig. 1. Here σ (Mie)/σ (Rayleigh) is plotted against α for various wavelengths. We shall define the ' Rayleigh region for back-scatter ' as the region for which this ratio lies between $\frac{1}{2}$ and 2. It will be seen that for wavelengths up to 17 mm, the ratio stays within these limits up to about $\alpha = 1$, where it falls rapidly. However, at longer wavelengths the ratio first rises beyond 2 so that the region only extends to $\alpha = 0{\cdot}4$ or less.

At 17 mm wavelength, the Rayleigh region as defined here extends to 6 mm diameter and includes all normal raindrop sizes. At shorter wavelengths, the limit occurs at smaller diameters, so that at $\lambda = 3$ mm, only particles less than 1 mm diameter are inside it. At 3 cm wavelength, the region is also reduced, extending only to 3 mm diameter, but at $\lambda = 10$ cm it covers all raindrop sizes so that the approximate formula can be safely used on rain.

Data for ice, equivalent to those plotted in Fig. 1 for water, were not evaluated by Lowan. Ryde (1946), however, considers that the Rayleigh approximate expressions for ice may be used for values of α up to 0·5 with small error. This means that the Rayleigh expressions (12), (13) and (14) may be used to compute the back-scattering cross-section

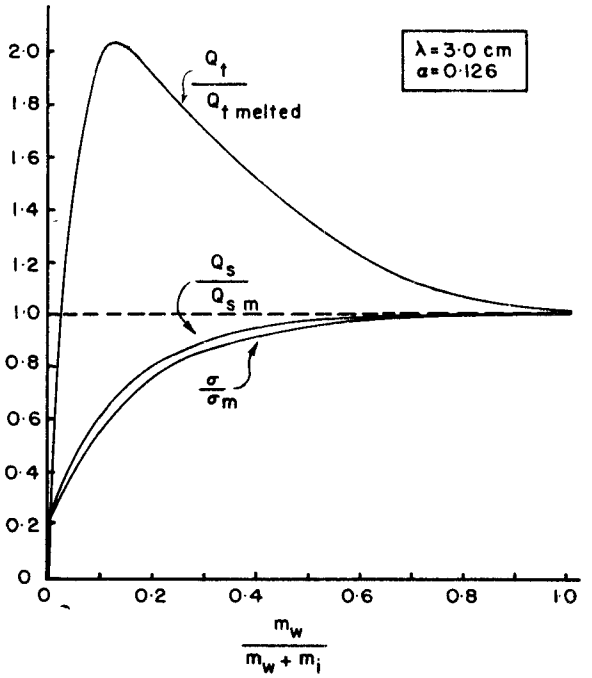

Figure 2. Attenuation, scattering and back-scatter cross-sections of water-coated ice sphere vs. proportion of water by mass. The cross-sections are relative to those for a water sphere of equal total mass.

and the attenuation for ice cloud at all centimetre wavelengths, and for single snow crystals probably down to wavelengths of 1·25 cm. Considering aggregate snowflakes as spherical (non-sphericity is found to be not too important, see Section 5 (a)), the Rayleigh approximate expressions can be applied at wavelengths down to about 5 cm for all except unusually large flakes. Scattering and attenuation from snow are discussed in Section 5.

(*d*) *Water-coated ice spheres*

Aden and Kerker (1951) extended Mie's theory to concentric spheres. Langleben and Gunn (1952) have applied this extended theory to spheres of ice coated with water in the region $\alpha < 1$. They consider a sphere, originally all ice, which changes gradually to ice coated with water, and finally entirely to water, maintaining constant mass. The calculated cross-sections for such a particle are plotted against the ratio of the mass of water to total mass in Fig. 2 for 3 cm wavelength and 1·2 mm initial diameter. As the thickness of the water coating increases from zero, the quantities σ, Q_s and Q_t all increase rapidly from their values for ice; when the sphere is still 70 per cent ice (so that the water thickness is less than one-tenth of the total radius) σ and Q_s are already nearly equal to those for the water sphere. Earlier still, Q_t reaches a maximum value, about twice as great as that for water. No simple explanation has been offered as yet for this extremely rapid increase of the attenuation to twice the value for pure water. For other wavelengths and diameters in the Rayleigh region, the curves for Q_s, σ and Q_t are very similar to those of Fig. 2. For larger values of α, the scattering cross-sections do not rise so early, and Q_t does not show such an extreme behaviour.

4. Rain

(a) *Drop-size distributions*

Where Rayleigh theory is applicable, radar can be used to measure the quantity $Z = \sum_1 D^6$, the sum of the sixth powers of the drop diameters in unit volume. A more significant quantity meteorologically is the rainfall rate, $R = \frac{\pi}{6} \rho \sum_1 (v_D D^3)$, where v_D is the terminal velocity of a drop of diameter D. To relate the two quantities the drop-size distribution must be observed. Distributions for rain at the ground have been determined in various parts of the world, for example, by Laws and Parsons (1943), Wexler (1948), Marshall and Palmer (1948), Best (1950), Hood (1950). Most of these workers have calculated simultaneous values of Z and R from the distribution of drop sizes obtained on a horizontal surface. Then from a number of such simultaneous values plotted on log-log paper a locus of best fit for the data of the form $Z = aR^b$ has been computed. There have been many such Z-R relations quoted in the literature in the past ten years, which give a wide range of Z values for a given R. Out of these, the authors have found ten relations which are based on measurements using original drop-size distribution data. These, along with pertinent information, are included in Table 3.

TABLE 3. Relations between Z and rainfall rate

$Z = aR^b$	Author	Location of observations	Ranges of rainfall rates treated	Number of Z-R values	How locus determined
$290\ R^{1.41}$	Blanchard (1953)	Hawaii	0·28 to 127 mm hr^{-1}	28	least squares fit
$208\ R^{1.58}$	Wexler (1948) on Anderson *et al.* (1947) data	Hawaii	7 to 50 mm hr^{-1}	49	least squares fit
$269\ R^{1.43}$	Mt. Washington Observatory (1951)	Cambridge, Mass.	0·07 to 87·5 mm hr^{-1}	63	least squares fit
$214\ R^{1.66}$	Wexler (1948) on Laws and Parsons' (1943) original data	Washington, D.C.	0·37 to 114 mm hr^{-1}	98	least squares fit
$200\ R^{1.6}$	Revised from Marshall and Palmer (1948)	Ottawa	0·15 to 35 mm hr^{-1}	250	best fit by eye (with a check to centre locus amongst data at that slope)
$295\ R^{1.41}$	Hood (1950)	Ottawa	0·5 to 60 mm hr^{-1}	270	best fit by eye
$505\ R^{1.44}$	Best (1950)	Shoeburyness	0·18 to 4·2 mm hr^{-1}	90	from analysis of mean distributions
$257\ R^{1.48}$	Best (1950)	Ynyslas	0·36 to 8.9 mm hr^{-1}	299	
$436\ R^{1.64}$	Best (1950)	East Hill	0·41 to 25·1 mm hr^{-1}	149	
$127\ R^{1.29}$	Twomey (1953)	Sydney, Australia	0·2 to 9 mm hr^{-1}	34	least squares fit

The number of points used to make up the different loci varies from one worker to another as does the range of rainfall rates covered. The great majority of the points in each case lie between 1 and 10 mm hr^{-1}.

The first six relations, obtained in North America lie within a factor 1·55 of the locus $Z = 244\ R^{1.55}$. The next three, obtained from measurements made in Great Britain, lie within a factor 1·59 of the locus $Z = 376\ R^{1.50}$. These nine relations are included within a band, a factor 1·70 either way from the locus

$$Z = 353\ R^{1.52} \quad . \quad . \quad . \quad . \quad (16)$$

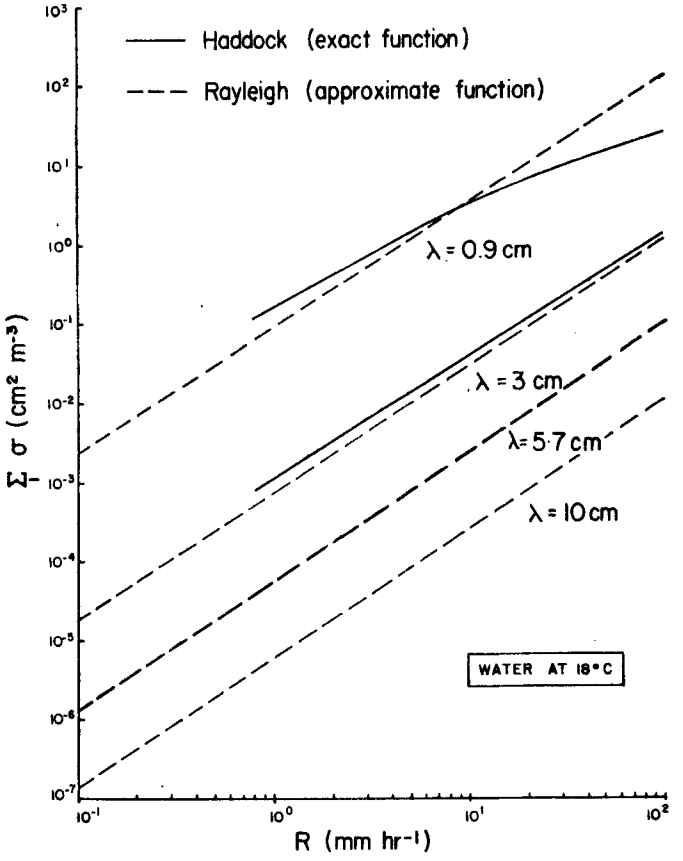

Figure 3. Exact and approximate (Rayleigh) back-scattering cross-sections per unit volume of rain-filled space, plotted against rainfall intensity.

The tenth relation $Z = 127\,R^{2\cdot29}$, reported by Twomey (1953) from measurements in Australia, departs considerably from the nine others, with a much steeper slope. His locus is based on relatively few data and while it does pass through the region defined by Eq. (16) in the important rainfall rate range 1-10 mm hr^{-1}, its departure at other rainfalls indicates the difficulty of giving a universal Z-R relation for all locations.

Any one of these loci represents only the average relationship at that particular place. Quite apart from scatter due to sampling methods which could easily amount to a factor 1·5 either way, the size distribution for a given R undoubtedly varies from one sample to another. Thus if one uses an average relationship such as Eq. (16), it is probably good to no better than a factor 2 or 3 either way. Unless one takes the variation during a rainfall and from one location to another into account, this uncertainty has to be accepted.

(*b*) *Scattering by rain*

The curves in Fig. 1 showed the behaviour of the exact back-scattering cross-sections for single drops. Haddock, in Plate 6 of his unpublished report, has evaluated the exact cross-sections for rain of various intensities using the drop-size distribution results of Laws and Parsons (1943). Haddock's data for back-scattering have been replotted in Fig. 3 which shows $\Sigma_1 \sigma$ against rainfall rate for two wavelengths, 3 cm and 0·9 cm. For

comparison, the Rayleigh approximate back-scattering cross-sections are shown for these same wavelengths. They are derived from summing Eq. (12) over unit volume and substituting $\sum_1 D^6 = 200\,R^{1\cdot6}$.

Haddock does not give a plot of the exact $\sum_1 \sigma$ for wavelengths greater than 3 cm, but the 5·7 and 10 cm curves will be identical with the Rayleigh one at all but the very heaviest rainfalls. At 0·9 cm, the exact back-scattering cross-section is larger than the Rayleigh for low rainfalls; it is the same at a rainfall of about 10 mm hr^{-1} and then becomes less quite quickly at higher rainfalls, being some 7·5 db below the Rayleigh value at 100 mm hr^{-1}. This rapid divergence of the two functions at 0·9 cm for heavy rainfalls is due to the rapid descent of the σ-curve for that wavelength (Fig. 1), at values of α which correspond to raindrop diameters. However, wavelengths shorter than 3 cm are not very useful for rain observations because of attenuation. At 3 cm wavelength, the appropriate values of α are somewhat lower, so that the difference between the exact curve and the Rayleigh curve does not exceed 2 db.

The curves of Fig. 3 are for a temperature of 18°C. In the Rayleigh region, temperature change will not affect the scattering greatly, since the quantity $|K|^2$ to which the scattering is proportional does not vary by more than a few per cent. Out of the Rayleigh region, the scattering is a more complex function of the refractive index, but according to Ryde (1946) the temperature effect on scattering is still not more than a few per cent.

Several workers have performed experiments to confirm Eq. (3). Marshall, Langille and Palmer (1947) obtained proportionality between $\overline{P_r}$ and $\sum_1 D^6$ at 10 cm wavelength, but did not measure the absolute power level. Hooper and Kippax (1950) confirmed the wavelength dependence at 10 cm, 3 cm and 1·25 cm, and the proportionality to pulse length h. They also reported that the absolute value of received power averaged about 1 db above the theoretical value. Hood (1950) found the expected proportionality between $\overline{P_r}$ and $\sum_1 D^6$, but $\overline{P_r}$ was 3 or 4 db too low at 10 cm and 7 db too low at 3 cm. He attributed this to a fixed error in the radar calibration or in the method of measuring $\sum_1 D^6$. However, Austin and Williams (1951) calibrated a radar with a known spherical target, thus eliminating the need for power measurements, and still obtained results 4 to 10 db too low on rain at 10 cm. They also ascertained that Hooper and Kippax were measuring *peak* received powers instead of the *average* power $\overline{P_r}$, which must have been several decibels lower. Donaldson *et al.* (1953) working with a 1·25 cm radar, which was calibrated with a spherical target, have reported a 2·5 db discrepancy between $\overline{P_r}$ and $\sum_1 D^6$. Each of these experiments shows considerable scatter of data, so the experiments cannot be said to disagree significantly with each other. However, it does seem that they disagree with the theory, and no satisfactory explanation has been reached.

(*c*) *Attenuation by rain*

For rain, the Rayleigh approximation for attenuation only applies for wavelengths of 10 cm and longer. At the shorter wavelengths, the attenuation through rain is no longer given by Eq. (6), but depends explicitly on diameter as well as on water content.

The data published by Laws and Parsons have been used by Ryde (1945, 1946) and Haddock to compute the attenuation at various wavelengths by a given rate of rainfall. The authors have repeated some of Haddock's calculations, using Laws and Parsons' data as plotted by Rigby, Marshall and Hitschfeld (1954) and Haddock's ratio in Fig. 1.

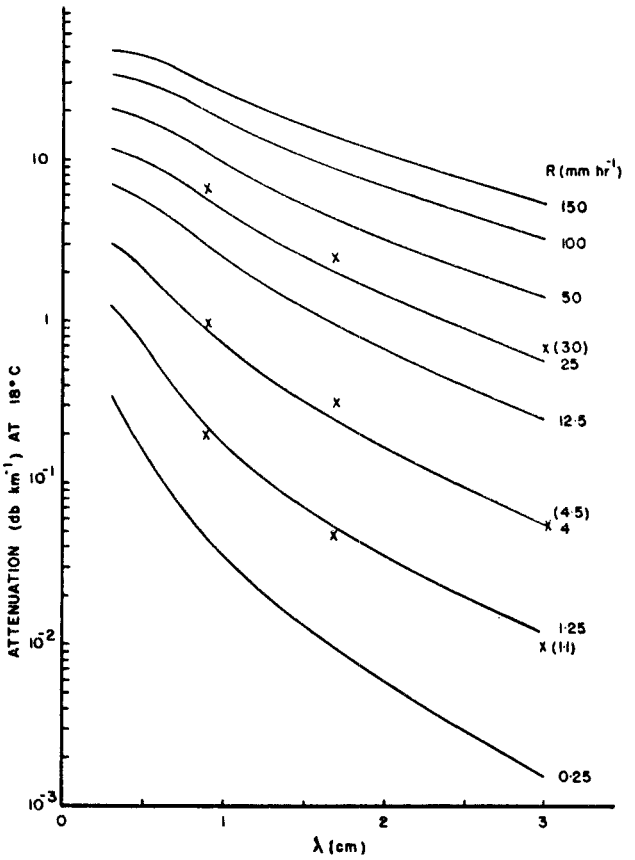

Figure 4. Attenuation versus wavelength for rainfall of various rates. Solid curves plotted from data in Haddock (1948); crosses are values computed by the authors.

In Fig. 4 these various calculated attenuations are plotted against wavelength for several rates of rainfall. Ryde's (1945) report shows good agreement with Haddock at rainfall rates above 12·5 mm hr^{-1} but his figures are up to 30 per cent greater at the lower rainfalls.

The results of Fig. 4 are replotted in Fig. 5. Here the abscissa is rainfall rate in mm/hr and the ordinate is attenuation divided by rainfall rate. The curve for 10 cm is plotted from Ryde's (1945) report; he gives no figures for wavelengths between 3·2 cm and 10 cm so the curve for 5·7 cm was obtained by graphical interpolation of his results. This process may have introduced an error of about 20 per cent. The dashed lines are the result of applying the Rayleigh approximation (Eq. 6). The ordinate in this diagram is the factor k in Ryde's (1946) Section 7; he suggests that, for many purposes, it may be taken as constant for a given wavelength. At 10 cm, k is very nearly constant, but has such a small value that it is negligible for radar purposes. At 5·7 cm, k increases slowly with rainfall rate; $k = 0{\cdot}003$ is an average figure, the empirical equation $k = 0{\cdot}0022\,R^{0{\cdot}17}$ fits more closely. At 3 cm, k is by no means constant and can be represented reasonably well by the empirical relation $k = 0{\cdot}009\,R^{0{\cdot}3}$, where R is the rainfall rate in mm hr^{-1}. However, if the rainfall rate is known to lie in a restricted range on any particular occasion, a suitable mean value for k could be used. At 9 mm, k is very nearly constant again, although it is 5 to 10 times the corresponding Rayleigh value. This is because the ratio plotted in Fig. 1 is near its maximum for these drop

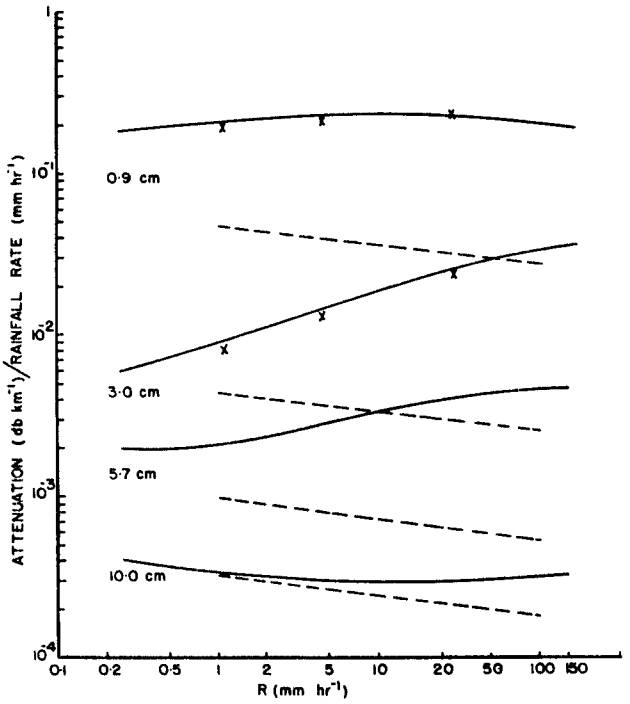

Figure 5. Attenuation/rainfall rate versus rainfall rate for various wavelengths. The solid curves are taken from Haddock (1948) for 0·9 and 3·0 cm, from Ryde (1945) for 10 cm. The curve at 5·7 cm is interpolated from Ryde's data. Dashed lines show the Rayleigh approximation.

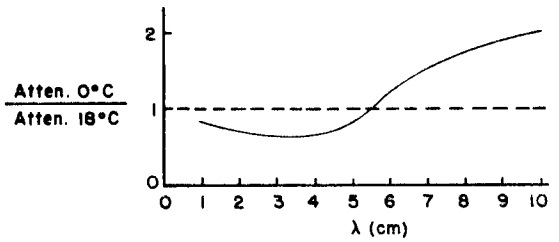

Figure 6. Approximate temperature correction curve for attenuation by rain (Fig. 7 of Ryde (1946)). For exact corrections at various rainfall rates, see Ryde (1945).

sizes at this wavelength. Whenever k can be taken as constant, the attenuation in db over the path is simply k times the integral of rainfall rate along the path in km-mm hr^{-1}.

Since the refractive index of water varies with temperature, the attenuation does also. In the Rayleigh region, attenuation is proportional to $Im\,(-K)$ and roughly doubles in value in going from 18°C to 0°C. Outside the Rayleigh region, to determine the attenuation at a temperature other than 18°C, it is necessary to have a set of curves of Q_t (Mie)/Q_t (Rayleigh), similar to those of Fig. 1 for the refractive indices of water at the required wavelengths at the new temperature. This involves lengthy computations, which Ryde (1945) carried out for a number of temperatures. Surprisingly, the attenuation at wavelengths less than 5·5 cm decreases in going from 18°C to 0°C. Ryde used the refractive index values quoted by Saxton and Lane (1946). The present authors made approximate calculations using the more recent values of Lane and Saxton (1952) which

also gave a decrease at these wavelengths; but only of about 10 per cent as opposed to Ryde's 30 per cent. Ryde's (1946) approximate correction curve which applies to rainfall rates greater than 2·5 mm hr^{-1} is shown in Fig. 6.

A number of point-to-point attenuation measurements have been made. Robertson and King (1946) measured attenuation at 1·09 and 3·2 cm wavelength in rainfalls from 2 to 100 mm hr^{-1}; their results show good agreement with Haddock's data, except below about 10 mm hr^{-1}, where measurements become inaccurate. Mueller (1946), at 0·62 cm, made similar measurements which are everywhere within 10 per cent of the theoretical values. The attenuations measured by Anderson, Day, Freres and Stokes (1947) in Hawaiian orographic rain at 1·25 cm are consistently greater than predicted values by factors of from 1·5 to 2. This may be due to drop-size distributions which differ markedly from those of Laws and Parsons. This seems a possible explanation in view of the remarkably large median diameters quoted by Anderson *et al.*, though Wexler (1948) found that their data gave a Z-R relationship similar to that computed from Laws and Parsons data (Table 3).

(*d*) *Distorted raindrops*

Photographs of water drops falling through stagnant air taken by Magono (1954) in the laboratory show that the bottom of a falling drop is always flattened (for drops of equivalent spherical diameter 2 mm and more) and the larger the drops the flatter the shape. Similar flattening has been observed in the few photographs so far taken of actual falling raindrops (Jones and Dean 1953). Experiments by Blanchard (1948) have shown that when a large drop catches up and collides with a smaller one it will oscillate about an equilibrium shape. Such oscillations can also occur as a result of aerodynamic forces on the drop as it falls. At any time, therefore, a fraction of the total number of drops in the contributing region is non-spherical. Stevenson (1953a, b) has recently published a theory of scattering by ellipsoids analogous to Mie's theory for spheres, and finds that for spheroids the scattered field can be expressed as a convergent series in α involving only elementary functions of the refractive index and of the geometry of the problem. This work has not yet been applied to calculations of Q_t and σ for non-spherical particles. An approximate theory for small spheroids which is analogous to the Rayleigh approximation has been used by Atlas, Kerker and Hitschfeld (1953) however, and they find that the flattening diminishes scattering and attenuation with vertical polarization and enhances it with horizontal polarization.

This effect cannot account for the difference between measured and predicted average received power because the observations were made with horizontally polarized radars, which would lead to greater measured powers rather than smaller.

5. Snow

(*a*) *Scattering by snow*

Dry snow consists of ice crystals, either single or aggregated. Calculations by Atlas, Kerker and Hitschfeld (1953) and by Labrum (1952b) on spheroids indicate that even considerable departures from sphericity are unimportant in the case of ice particles, the cross-sections never being more than twice as great as those for spheres of the same mass. Since the refractive index for ice is less than that of water, the factor $|K|^2$ to which scattering in the Rayleigh region is proportional, is about 0·22 times that for a water sphere of the same mass.

Aggregate snowflakes consist of a mixture of air and ice of low mean density. It can be shown (Marshall and Gunn 1952) that K/ρ is the same as that for the same mass

of ice in compact form. This means that, for snowflakes small enough for the Rayleigh approximation to apply, $\sum_1 \sigma$ can be calculated by catching a sample of snow flakes, melting them, measuring $\sum_1 D^6$ for the resulting drops and allowing for the dielectric factor.

This was done by Langille and Thain (1951) who also made radar measurements at the same time. The agreement with the form of Eq. (1) was within the scatter of the observations, but the received power was 4 db less than predicted. As in the rain measurements, this difference is unexplained. Langille and Thain's results, on further analysis (Marshall and Gunn 1952), yield an empirical relation between Z and R, where Z refers to unit volume of snowstorm and is the sum of the sixth powers of the diameters of the drops formed from the melted flakes, and R is the snowfall rate at the ground measured in millimetres of water per hour. The overall relation is $Z = 200\,R^{1\cdot6}$, identical with the Canadian results for rain*. Since the reflectivity of ice is 0·22 times that of water, radar echoes from snow are 0·22 times those from rain of the same rainfall rate.

(b) *Attenuation by snow*

Attenuation by snow will be partly due to scattering and partly due to absorption of the incident energy (Section 3 (b)).

According to Eqs. (5) and (15)

$$\text{attenuation (db km}^{-1}) = 0\cdot4343 \sum_1 Q_t$$
$$= 0\cdot4343 \left(\sum_1 Q_s + \sum_1 Q_a \right).$$

We can use the approximate expressions (13) and (14) if the wavelength is long compared to the particle diameters; the values of $|K|^2$ and $Im\,(-K)$ which apply are listed in Table 2 and are based on Cumming's (1952) values. This gives

$$\text{attenuation at 0°C (db km}^{-1}) = 0\cdot00349 \frac{R^{1\cdot6}}{\lambda^4} + 0\cdot00224 \frac{R}{\lambda}. \quad . \quad (17)$$

Ryde (1946) suggests that attenuation by snow in the Rayleigh region and at centimetric wavelengths is given by the second term only. In Table 5, values of the attenuation calculated from Eq. (17) for 3 temperatures show that the first term (scattering) is indeed negligible at 10 cm but becomes increasingly important on going to shorter wavelengths.

(c) *Wet snow and the 'bright band'*

Atlas, Kerker and Hitschfeld (1953) show that randomly-oriented small water spheroids scatter and attenuate more strongly than water spheres of the same volume; for example, the increase is by a factor of 20 or more if the length of each spheroid is 10 times its diameter. Labrum (1952b) has computed the scattering by an ice ellipsoid coated with water for wavelengths large compared with the size of the particle (corresponding to the Rayleigh approximation for spheres). He showed that even for comparatively thin coatings the composite particle should scatter nearly as well as an all-water particle of the same shape. In a subsequent experiment, he confirmed this result (Labrum 1952a).

Extrapolating from the results of Labrum for small water-coated ice spheroids, of Langleben and Gunn (1952) for larger water-coated spheres and the above-mentioned

* Despite the higher concentration (about 5 times) of snow particles caused by their lower fall velocities. This implies an increase in average particle mass at or about the level of melting.

shape effects for water, it seems reasonable to assume that the scattering and attenuation by water-coated ice spheroids of the size of wet snowflakes at radar wavelengths is similar in magnitude to that of spheroidal water drops of the same shape and size.

This is relevant to the bright band which always appears in radar pictures of steady rain. The bright band is due to a region of enhanced reflectivity a few hundred feet thick just below the 0°C isotherm. In the light of the foregoing discussion, the following mechanism is suggested. Snow falling through the freezing level will change from flat or needle-shaped particles or aggregates which scatter feebly, to similarly-shaped particles, which, owing to a water coating, scatter relatively strongly. As melting proceeds, they lose their extreme shapes and the shape factor decreases to unity. Because of the greater velocity of fall, the number of particles in unit volume also becomes less.

Evidence of shape effects in the bright band has been obtained from observations with cross-polarized radars (Browne and Robinson 1952; Hunter 1954). Non-spherical particles can scatter back power with different polarization from that transmitted. The topic is discussed more fully by Marshall, Hitschfeld and Gunn (1954).

Attenuation, like scattering, is proportional to the number of particles per unit volume, and therefore depends on the velocity of fall. Water spheroids absorb more strongly than water spheres, and coated ice spheroids presumably absorb like water spheroids. Therefore, absorption by melting snow will be many times that of the resulting rain. Although the bright band is comparatively thin, serious attenuation may take place when radar observations are made through it at shallow elevations.

6. Clouds

Most cloud droplets do not exceed 100 μ diameter, so that at centimetre and millimetre wavelengths the Rayleigh formulae (12) and (14) apply for droplets and Eqs. (3) and (6) for cloud.

(*a*) *Scattering from clouds*

Cloud droplets being about one-hundredth the diameter of raindrops, $\sum_1 D^6$ in cloud is about a factor 10^6 less than in rain. However, Eq. (3) for the received power has λ^4 in the denominator, so that it is possible to overcome some of the effect of the very small diameters by going to the shortest practicable wavelength. Radar sets working on wavelengths of 1·25 cm and around 9 mm are now being used for cloud observations (Plank, Atlas and Paulsen 1952; Swingle 1953). By directing the antenna vertically, the range r is made a minimum, and most clouds visible to the eye are detected by the receiver.

The radar signal is proportional to $Z = \sum_1 D^6$. To relate Z to other significant quantities such as liquid water content $M \left(= \frac{\pi}{6} \rho \sum_1 D^3\right)$ would require the complete drop-size distribution. However, Atlas and Bartnoff (1953), after studying a number of such distributions actually observed in clouds, report that a knowledge of the median diameter only is sufficient for a fairly accurate relationship, since the shape of the distribution is similar for all clouds. Even without this knowledge, an approximate correlation between Z and M can be obtained (Atlas and Boucher 1952) because the median diameter shows a definite trend with M, and this can be incorporated in the empirical law

$$Z = 0{\cdot}0292\, M^{1{\cdot}82},$$

where M is in gm m^{-3}, and Z in mm^6 m^{-3}.

Donaldson *et al.* (1953) have recently made simultaneous measurements at 1·25 cm of scattered power and size distributions in fog. A preliminary analysis gives received powers 10 db below the theoretical values; the work is not yet sufficiently advanced to say whether or not this discrepancy can be accounted for by the measuring techniques.

(*b*) *Attenuation by clouds*

Since the cloud particles lie well within the Rayleigh region at all wavelengths in the centimetre band, Eq. (6) applies :

$$\text{attenuation (db km}^{-1}) = 0{\cdot}4343\,\frac{6\pi}{\lambda}\,\frac{M}{\rho}\,Im\,(-K) \qquad . \qquad . \qquad (6)$$

for one-way transmission. Thus attenuation by cloud depends on the liquid-water content and is independent of the particle-size distribution.

Values of the attenuation from water and ice clouds are given in Table 5 as a function of M for six wavelengths and three temperatures. For both ice clouds and water clouds $Q_s \ll Q_a$.

7. Concluding remarks

(*a*) *Refractive indices*

The measured values of the refractive index of water for various wavelengths and temperatures are quite adequate for microwave-precipitation work. The fact that the measured values fit the theoretical formulae so well (see, for example, Saxton and Lane 1946) allows interpolation and extrapolation about these values to be made with confidence.

The situation for ice is not so well established. There is agreement on the value of the real part of the refractive index and on its independence of temperature and wavelength in the microwave region. However, measured values of the imaginary part differ by a factor 2. Further determinations of this quantity are desirable.

(*b*) *Rain*

Drop-size distributions continue to be measured, both as an adjunct of scattering and attenuation measurements and independently, but they will probably not make much impression on the universal relationship of Eq. (16). Some understanding of the variation of drop-size distributions with time is now being acquired (Atlas and Plank 1953; Marshall 1953) which should make it easier to relate the radar signal to parameters measured at the ground.

Though Ryde (1945) evaluated the attenuation by rain at four wavelengths, and various temperatures, the work may bear repeating for the slightly changed values of the refractive index of water which have been reported since his computations were made, at least at 0°C, although the final results may not be very different.

One outstanding unsolved problem is the source of the 4-7 db difference between the actual signal received from both rain and snow and that predicted from the theory.

(*c*) *Snow*

Labrum (1952a) has observed the scattering from single melting spheroidal ice particles, but there has been little experimental work done on either scattering or attenuation by falling snow. There is a need for laboratory experiments to study the melting of natural snowflakes, both single crystals and aggregates. Point-to-point measurements of attenuation by melting snow would be particularly valuable.

(*d*) *Summary*

By way of summarizing, the back-scatter cross-sections per unit volume and the attenuation to be expected from rain, snow, water cloud and ice cloud for six wavelengths and various temperatures are shown in Tables 4 and 5.

When two or more of the elements listed in these Tables (and in Table 6, Appendix I) are present, the cross-sections and attenuations are additive. In a typical case, the attenuation in decibels will be the sum of the attenuations by rain, cloud and atmosphere.

TABLE 4. BACK-SCATTER CROSS-SECTION PER UNIT VOLUME $\sum_1 \sigma$ IN $CM^2\ M^{-3}$

	T (°C)	$\lambda = 10$ cm	$\lambda = 5{\cdot}7$ cm	$\lambda = 3{\cdot}2$ cm	$\lambda = 1{\cdot}8$ cm	$\lambda = 1{\cdot}24$ cm	$\lambda = 0{\cdot}9$ cm
Rain* R in mm hr^{-1}	18	$5{\cdot}89 \times 10^{-6} R^{1{\cdot}6}$	$5{\cdot}59 \times 10^{-5} R^{1{\cdot}6}$	$8{\cdot}4 \times 10^{-4} R^{1{\cdot}56}$			$0{\cdot}16 R^{1{\cdot}38}$
Snow R in mm hr^{-1} of melted water	All Temps	$1{\cdot}21 \times 10^{-6} R^{1{\cdot}6}$	$1{\cdot}15 \times 10^{-5} R^{1{\cdot}6}$	$1{\cdot}15 \times 10^{-4} R^{1{\cdot}6}$	$1{\cdot}15 \times 10^{-3} R^{1{\cdot}6}$	Rayleigh approximations no longer applicable	
Water cloud M in gm m^{-3}	20	$8{\cdot}29 \times 10^{-4} M^{1{\cdot}82}$	$7{\cdot}86 \times 10^{-3} M^{1{\cdot}82}$	$7{\cdot}91 \times 10^{-2} M^{1{\cdot}82}$	$0{\cdot}785 M^{1{\cdot}82}$	$3{\cdot}74 M^{1{\cdot}82}$	$12{\cdot}4 M^{1{\cdot}82}$
	10	$8{\cdot}32 \times 10^{-4} M^{1{\cdot}82}$	$7{\cdot}88 \times 10^{-3} M^{1{\cdot}82}$	$7{\cdot}91 \times 10^{-2} M^{1{\cdot}82}$	$0{\cdot}783 M^{1{\cdot}82}$	$3{\cdot}46 M^{1{\cdot}82}$	$12{\cdot}3 M^{1{\cdot}82}$
	0	$8{\cdot}34 \times 10^{-4} M^{1{\cdot}82}$	$7{\cdot}89 \times 10^{-3} M^{1{\cdot}82}$	$7{\cdot}93 \times 10^{-2} M^{1{\cdot}82}$	$0{\cdot}781 M^{1{\cdot}82}$	$3{\cdot}42 M^{1{\cdot}82}$	$12{\cdot}1 M^{1{\cdot}82}$
	− 8		$7{\cdot}92 \times 10^{-3} M^{1{\cdot}82}$ (extrapolated)	$7{\cdot}95 \times 10^{-2} M^{1{\cdot}82}$ (extrapolated)	$0{\cdot}778 M^{1{\cdot}82}$ (extrapolated)	$3{\cdot}36 M^{1{\cdot}82}$	$11{\cdot}6 M^{1{\cdot}82}$

* The Rayleigh approximations have been used at 10 and 5·7 cm; at 3·2 and 0·9 empirical relations based on the curves of Fig. 3 are given.

TABLE 5. ATTENUATION DUE TO PRECIPITATION OR CLOUD (ONE-WAY) IN DB KM^{-1}

	T (°C)	$\lambda = 10$ cm	$\lambda = 5{\cdot}7$ cm	$\lambda = 3{\cdot}2$ cm	$\lambda = 1{\cdot}8$ cm	$\lambda = 1{\cdot}24$ cm	$\lambda = 0{\cdot}9$ cm
Rain* R in mm hr^{-1}	18**	$0{\cdot}0003 R^{1{\cdot}00}$	$0{\cdot}0022 R^{1{\cdot}17}$	$0{\cdot}0074 R^{1{\cdot}21}$	$0{\cdot}045 R^{1{\cdot}14}$	$0{\cdot}12 R^{1{\cdot}05}$	$0{\cdot}22 R^{1{\cdot}09}$
Snow*** R in mm hr^{-1} of melted water	0	$0{\cdot}035 \times 10^{-5} R^{1{\cdot}6} + 22{\cdot}0 \times 10^{-5} R$	$0{\cdot}33 \times 10^{-5} R^{1{\cdot}6} + 38{\cdot}5 \times 10^{-5} R$	$3{\cdot}3 \times 10^{-5} R^{1{\cdot}6} + 68{\cdot}6 \times 10^{-5} R$	$33{\cdot}2 \times 10^{-5} R^{1{\cdot}6} + 122 \times 10^{-5} R$		
	− 10	$0{\cdot}035 \times 10^{-5} R^{1{\cdot}6} + 7{\cdot}3 \times 10^{-5} R$	$0{\cdot}33 \times 10^{-5} R^{1{\cdot}6} + 12{\cdot}9 \times 10^{-5} R$	$3{\cdot}3 \times 10^{-5} R^{1{\cdot}6} + 22{\cdot}9 \times 10^{-5} R$	$33{\cdot}2 \times 10^{-5} R^{1{\cdot}6} + 40{\cdot}6 \times 10^{-5} R$	Rayleigh approximations no longer applicable	
	− 20	$0{\cdot}035 \times 10^{-5} R^{1{\cdot}6} + 5{\cdot}0 \times 10^{-5} R$	$0{\cdot}33 \times 10^{-5} R^{1{\cdot}6} + 8{\cdot}8 \times 10^{-5} R$	$3{\cdot}3 \times 10^{-5} R^{1{\cdot}6} + 15{\cdot}7 \times 10^{-5} R$	$33{\cdot}2 \times 10^{-5} R^{1{\cdot}6} + 28{\cdot}0 \times 10^{-5} R$		
Water cloud M in gm m^{-3}	20	$0{\cdot}39 \times 10^{-3} M$	$1{\cdot}36 \times 10^{-3} M$	$4{\cdot}83 \times 10^{-3} M$	$12{\cdot}8 \times 10^{-3} M$	$31{\cdot}1 \times 10^{-3} M$	$64{\cdot}7 \times 10^{-3} M$
	10	$0{\cdot}56 \times 10^{-3} M$	$1{\cdot}96 \times 10^{-3} M$	$6{\cdot}30 \times 10^{-3} M$	$17{\cdot}9 \times 10^{-3} M$	$40{\cdot}6 \times 10^{-3} M$	$68{\cdot}1 \times 10^{-3} M$
	0	$0{\cdot}90 \times 10^{-3} M$	$2{\cdot}72 \times 10^{-3} M$	$8{\cdot}58 \times 10^{-3} M$	$26{\cdot}7 \times 10^{-3} M$	$53{\cdot}2 \times 10^{-3} M$	$99 \times 10^{-3} M$
	− 8		$3{\cdot}4 \times 10^{-3} M$ (extrapolated)	$11{\cdot}2 \times 10^{-3} M$ (extrapolated)	$34 \times 10^{-3} M$ (extrapolated)	$68 \times 10^{-3} M$	$125 \times 10^{-3} M$
Ice cloud M in gm m^{-3}	0	$7{\cdot}87 \times 10^{-4} M$	$13{\cdot}8 \times 10^{-4} M$	$24{\cdot}6 \times 10^{-4} M$	$43{\cdot}6 \times 10^{-4} M$	$63{\cdot}5 \times 10^{-4} M$	$87{\cdot}4 \times 10^{-4} M$
	− 10	$2{\cdot}62 \times 10^{-4} M$	$4{\cdot}60 \times 10^{-4} M$	$8{\cdot}19 \times 10^{-4} M$	$14{\cdot}6 \times 10^{-4} M$	$21{\cdot}1 \times 10^{-4} M$	$29{\cdot}3 \times 10^{-4} M$
	− 20	$1{\cdot}80 \times 10^{-4} M$	$3{\cdot}16 \times 10^{-4} M$	$5{\cdot}63 \times 10^{-4} M$	$10{\cdot}0 \times 10^{-4} M$	$14{\cdot}5 \times 10^{-4} M$	$20{\cdot}0 \times 10^{-4} M$

* These are empirical relations. For the curves on which they are based see Fig. 5.

** The effect of temperature on attenuation by rain is discussed in Section 4 (c).

*** These values are obtained using the Rayleigh approximations, which are not valid for wavelengths less than about 1·5 cm. A value of $R = 10$ or $R^{1{\cdot}6} = 39$ is an upper limit for snowfall rates.

ACKNOWLEDGMENT

The authors wish to express their thanks to Professor J. S. Marshall for his advice and many constructive suggestions.

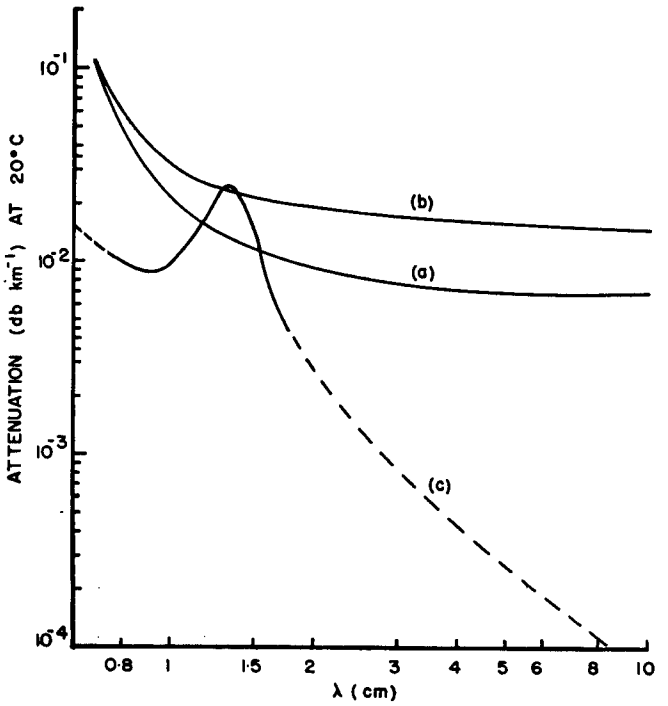

Figure 7. Atmospheric attenuation versus wavelength. (a) Attenuation due to O_2 in air at 1 atmos pressure and 293°K, using $\Delta\nu = 0{\cdot}039$ cm^{-1} for 5 mm lines and $\Delta\nu = 0{\cdot}02$ cm^{-1} for zero-frequency line. (b) As (a), using $\Delta\nu = 0{\cdot}039$ cm^{-1} for 5 mm lines and $\Delta\nu = 0{\cdot}05$ cm^{-1} for zero-frequency line. (c) Attenuation due to 1 g m^{-3} of water vapour in atmosphere : full line, measured (Becker and Autler 1946); dashed line, calculated. Attenuation is approximately proportional to water vapour content.

Appendix I

Attenuation by atmospheric gases

Eq. (7) does not take account of absorption by atmospheric gases. It has been shown by infra-red and, more recently, by microwave spectroscopy that oxygen molecules have a magnetic dipole moment and water-vapour molecules have an electric dipole moment. These give rise to lines in the absorption spectra which lie in the centimetre and millimetre region. This means that radar propagation is subject to attenuation by oxygen and water vapour in the atmosphere. Van Vleck (1947a, b) has discussed the problem in detail. He points out that these absorption lines are subject to the usual amount of 'pressure broadening.' In water vapour, under atmospheric conditions, the most important line has a line breadth (from resonance to half-intensity) of about 0·1 cm^{-1}. Since the wave-number of the line itself is only 0·74 cm^{-1} the line is relatively very broad; it has a resonant wavelength of 1·348 cm and its influence extends from about 1 cm to 2 cm wavelength. Additional effects are found due to other, much stronger, absorption lines centred near 0·2 cm wavelength.

Becker and Autler (1946) measured the damping of a large cavity resonator filled with air and water vapour. They used wavelengths between 0·75 cm and 1·7 cm. Their results are plotted as part of curve (c) in Fig. 7. The experiments were performed at 45°C, but have been corrected to 20°C in plotting the curve to bring it into line with the other curves. The dashed portions of curve (c) are calculations by Van Vleck from a theoretical formula with the constants chosen to fit Becker and Autler's results. Curve (c) is drawn for one gm m^{-3}, and attenuation is approximately proportional to water vapour content for the amounts encountered in the atmosphere. Dicke, Beringer, Kyhl and

Vane (1946) used a radiometer method to investigate absorption by atmospheric water vapour at 1·0 cm, 1·25 cm and 1·5 cm. Though the accuracy is not high, their results are consistent with those of Becker and Autler.

The situation for oxygen differs in two respects from that for water vapour; the most important absorption is caused by a number of closely-spaced lines instead of a single line and, in addition, oxygen has a line at zero frequency, while water vapour has not.

There are about 25 absorption lines between 0·45 and 0·56 cm wavelength; their positions were first predicted by Van Vleck and have been measured in pure oxygen at low pressures by Burkhalter, Anderson, Smith and Gordy (1950) and by Anderson, Smith and Gordy (1952). The later work included line breadth measurements which show values varying from line to line between $\Delta\nu = 0{\cdot}0319$ and $0{\cdot}0516$ cm^{-1}/atmos for pure oxygen*. An average value weighted for line intensity, and reduced by 18 per cent to allow for the difference in collision cross-section between pure oxygen and air, is $\Delta\nu = 0{\cdot}039$ cm^{-1}/atmos for air.

At atmospheric pressure this amount of broadening converts the line spectrum into an unresolved band of absorption. Lamont (1948) measured attenuation in air at wavelengths between 0·45 and 0·58 cm over a path of a few kilometres in the field. Between 0·5 and 0·53 cm the attenuation averaged 13 db km^{-1}; his results are in fair agreement with the theory extrapolated from low pressures.

Van Vleck's predictions include a ' line ' at zero frequency, and this accounts for most of the attenuation at wavelengths from 1 cm upwards**. The contribution of this ' line ' to the attenuation is independent of wavelength (for wavelengths shorter than 10 cm) and proportional to line breadth. No measurement appears to have been made above 0·6 cm specifically on oxygen, so that the line breadth for the zero-frequency line is not known with any certainty and the whole curve above 1 cm is in doubt. The radiometer measurements of Dicke *et al.* at 1·0 to 1·5 cm can be extrapolated back to zero water content, and indicate an absorption by oxygen corresponding to line breadth for zero frequency of $\Delta\nu = 0{\cdot}02$ cm^{-1}/atmos. The spread of the data, however, is large enough to make this figure very uncertain, and one can say little more than that the line breadth cannot be very much greater than this amount. Van Vleck (1947a) mentions a measurement by Mueller which indicates the same thing.

At the time that Van Vleck's calculations were made, it was believed that the line breadth constant $\Delta\nu$ was the same from line to line, though its value was not known. Accordingly, he assigned several alternative values to $\Delta\nu$ and the predicted attenuation for $\Delta\nu = 0{\cdot}02$ cm^{-1}/atmos and $\Delta\nu = 0{\cdot}05$ cm^{-1}/atmos (two likely values) were used by Ryde (1946) in his Fig. 1, curves (a) and (b).

Since so little is known, even at this date, about the zero-frequency line, in Fig. 7 we have used the same two values, viz. $\Delta\nu = 0{\cdot}02$ cm^{-1}/atmos, the most probable value, and $\Delta\nu = 0{\cdot}05$ cm^{-1}/atmos, which is to be taken as an upper limit, for the zero-frequency line together with the new, fairly reliable value $\Delta\nu = 0{\cdot}039$ for the 0·5 cm lines.

A laboratory experiment at any wavelength over 1 cm on dry air at atmospheric and at very low pressures, or a field experiment at any wavelength over 3 cm at a low humidity would determine the line-breadth constant and remove the uncertainty at wavelengths above the 0·5 cm band. However, since the attenuation appears to be not much greater than 0·01 db km^{-1} it is difficult to measure and at the same time usually unimportant in practice. Any application in which it becomes important to know it precisely will probably suggest a way of measuring it accurately.

* Added in proof – Artman (' Absorption of microwaves by oxygen in the millimetre wavelength region,' *Columbia Radiation Lab. Rep.*, 1953) finds that the line breadth is very nearly constant for these lines and that under atmospheric conditions it is 0·039 cm^{-1}/atmos.

** An alternative approach to this kind of absorption can be made by using Debye's theory of polar molecules in dielectrics.

The pressure and temperature dependence of attenuation are discussed by Van Vleck in his two papers. For a given quantity of water vapour, attenuation is proportional to p^{-1} and to $T^{-2}\,10^{-278/T}$ at the maximum of the resonance curve, to p and to $T^{-3}\,10^{-278/T}$ on the sides of the curves, and to p and to $T^{-3/2}$ well away from the resonance. Of course, if the air is kept saturated with water vapour while the temperature changes, the water vapour content itself will alter, and this additional factor must be taken into account. In these expressions T is in degrees Kelvin.

Table 6 shows attenuation by water vapour in air at various temperatures and wavelengths.

Pressure effect on atmospheric oxygen arises from increased pressure broadening and also from an increase in the number of molecules per unit volume. In the region of strong absorption, the attenuation is more or less independent of p and proportional to $T^{-3/2}$, but in the region from 0·7 to 10 cm wavelength it is proportional to p^2 and to $T^{-5/2}$.

Table 7 shows correction factors by which values read from curves (a) and (b) of Fig. 7 should be multiplied to obtain attenuation in conditions other than 20°C and 76 cm Hg.

TABLE 6. WATER VAPOUR ATTENUATION (ONE WAY) IN DB KM^{-1}

P, pressure in atmospheres; W, water vapour content in g m^{-3}.

	λ (cm)					
T (°C)	10·0	5·7	3·2	1·8	1·24	0·9
20	$0{\cdot}07 \times 10^{-3}\,PW$	$0{\cdot}24 \times 10^{-3}\,PW$	$0{\cdot}7 \times 10^{-3}\,PW$	$4{\cdot}3 \times 10^{-3}\,PW$*	$22{\cdot}0 \times 10^{-3}\,P^{-1}\,W$*	$9{\cdot}5 \times 10^{-3}\,PW$
0	$0{\cdot}08 \times 10^{-3}\,PW$	$0{\cdot}27 \times 10^{-3}\,PW$	$0{\cdot}8 \times 10^{-3}\,PW$	$4{\cdot}8 \times 10^{-3}\,PW$*	$23{\cdot}3 \times 10^{-3}\,P^{-1}\,W$*	$10{\cdot}4 \times 10^{-3}\,PW$
− 20	$0{\cdot}09 \times 10^{-3}\,PW$	$0{\cdot}30 \times 10^{-3}\,PW$	$0{\cdot}9 \times 10^{-3}\,PW$	$5{\cdot}0 \times 10^{-3}\,PW$*	$24{\cdot}6 \times 10^{-3}\,P^{-1}\,W$*	$11{\cdot}4 \times 10^{-3}\,PW$
− 40	$0{\cdot}10 \times 10^{-3}\,PW$	$0{\cdot}34 \times 10^{-3}\,PW$	$1{\cdot}0 \times 10^{-3}\,PW$	$5{\cdot}4 \times 10^{-3}\,PW$*	$26{\cdot}1 \times 10^{-3}\,P^{-1}\,W$*	$12{\cdot}6 \times 10^{-3}\,PW$

* The pressure dependences shown here are only approximate. In the neighbourhood of the 1·35 cm water vapour absorption line (say between 1·0 cm and 2·0 cm) no simple power law is accurate.

TABLE 7. PRESSURE AND TEMPERATURE CORRECTION FOR OXYGEN ATTENUATION FOR WAVELENGTHS BETWEEN 0·7 AND 10·0 CM

T (°C)	Factor (P is pressure in atmospheres)
20	$1{\cdot}00\,P^2$
0	$1{\cdot}19\,P^2$
− 20	$1{\cdot}45\,P^2$
− 40	$1{\cdot}78\,P^2$

APPENDIX II

ERRORS NOTED IN THE LITERATURE OF SCATTERING AND ABSORPTION BY SPHERES

While consulting the published work on the scattering and absorption of electromagnetic waves by spheres, a number of typographical errors were noticed. It may serve a useful purpose to list them here, though this list does not claim to be complete.

Mie (1908). In the expansions of the Spherical Bessel functions, Eq. (27) on page 388 contains an error. The expression for $K_2(-x)$ should begin $-3/x^2$.

The three identities on page 437 are confusing because some of the symbols are printed in the wrong type; they can be clarified by referring to Eq. (93) on page 424. Later authors have used a different notation, but the relationships are fairly simple and are stated in Goldstein (1946), Eq. (39) on page 155.

Kerr (1951) states correctly the expansions of a_1, b_1, and b_2 on page 451, Eqs. (30a, b, c) (Eqs. (11a, b, c) in the present paper).

Goldstein (1946). On page 155, Eq. (38), the expression for b_1 should have a + sign before the ρ^2 term in the bracket; on page 171, it is given correctly.

Stratton (1941). P. 571, Eq. (40) has several errors. Goldstein (1946), page 155, has listed them in a footnote. He also mentions the following : a minus sign is missing in Stratton's Eqs. (26) for W_t and (29) and (31) for Q_t. At the top of the next page Q_s should equal Q_t. In Eq. (35) the denominator of the ρ^2 term should be $(2n + 2)(2n + 3)$, and in Eq. (36) there should be a minus sign.

Sinclair (1947) reviews various ways in which an incorrect factor 2 sometimes appears and explains the conditions under which the result $Q_t = 2\pi r^2$ for $\alpha \gg 1$ is correct.

References

Aden, A. L. and Kerker, M. 1951 ' Scattering of electromagnetic waves by two concentric spheres,' *J. Appl. Phys.*, **22**, p. 1242.

Anderson, L. J., Day, J. P., Freres, C. H. and Stokes, A. P. D. 1947 'Attenuation of 1·25 cm radiation through rain,' *Proc. Inst. Radio Engrs.*, **35**, p. 351.

Anderson, R. S., Smith, W. V. and Gordy, W. 1952 ' Line-breadths of the microwave spectrum of oxygen,' *Phys. Rev.*, **87**, p. 561.

Atlas, D. and Bartnoff, S. 1953 ' Cloud visibility, radar reflectivity and drop-size distribution,' *J. Met.*, **10**, p. 143.

Atlas, D. and Boucher, R. 1952 ' The relation of cloud reflectivity to drop-size distribution,' *Proc. Third Radar Weather Conf., McGill Univ.*, B-1.

Atlas, D., Kerker, M. and Hitschfeld, W. 1953 ' Scattering and attenuation by non-spherical atmospheric particles,' *J. Atmos. Terr. Phys.*, **3**, p. 108.

Atlas, D. and Plank, V. G. 1953 ' Drop-size history in a shower,' *J. Met.*, **10**, p. 291.

Austin, P. M. and Williams, E. L. 1951 ' Comparison of radar signal intensity with precipitation rate,' *Tech. Rep. M.I.T.* Dept. *Met.*, No. 14.

Becker, G. E. and Autler, S. H. 1946 ' Water vapour absorption of electromagnetic radiation in the centimetre wave-length range,' *Phys. Rev.*, **70**, p. 300.

Best, A. C. 1950 ' The size distribution of raindrops,' *Quart. J. R. Met. Soc.*, **76**, p. 16.

Blanchard, D. C. 1948 ' Observations on the behaviour of water drops at terminal velocity in air,' *G. E. Res. Lab.: Project Cirrus, Occasional Rep.*, No. 7.

1953 ' Raindrop size-distribution in Hawaiian rains,' *J. Met.*, **10**, p. 457.

Browne, I. C. and Robinson, N. P. 1952 ' Cross polarization of the radar melting band,' *Nature*, **170**, p. 1078.

Buchanan, T. J. 1952 ' Balance methods for the measurement of permittivity in the microwave region,' *Proc. Inst. Elect. Engrs.*, **99**, III, p. 61.

Burkhalter, J. S., Anderson, R. S., Smith, W. V. and Gordy, W. 1950 ' The fine structure of the microwave absorption spectrum of oxygen,' *Phys. Rev.*, **79**, p. 651.

Collie, C. H., Hasted, J. B. and Ritson, D. M. 1948 ' The dielectric properties of water and heavy water,' *Proc. Phys. Soc. Lond.*, **60**, p. 145.

Cumming, W. A. 1952 ' The dielectric properties of ice and snow at 3·2 cm,' *J. Appl. Phys.*, **23**, p. 768.

Debye, P. 1929 *Polar molecules*, New York (The Chemical Catalogue).

Dicke, R. H., Beringer, R., Kyhl, R. L. and Vane, A. B. 1946 'Atmospheric absorption measurements with a microwave radiometer,' *Phys. Rev.*, **70**, p. 340.

Donaldson, R. J., Atlas, D., Paulsen, W. H., Cunningham, R. M. and Chmela, A. C. 1953 ' Quantitative 1·25 cm observations of rain and fog,' *Proc. Conf. Radio Met. Univ. Texas*, VII-6.

Dunsmuir, R. and Lamb, J.	1945	' The dielectric properties of ice at wavelengths of 3 and 9 cm,' *Manchester Univ. Rept.*, No. 61.
Goldstein, L.	1946	' Radio wave propagation experiments,' Summary *Tech. Rep. Commit. Propagation, NDRC*, **2**, Washington,
Haddock, F. T.	1948	' Scattering and attenuation of microwave radiation through rain,' *Naval Res. Lab.*, Washington (unpublished manuscript).
Hood, A. D.	1950	' Quantitative measurements at 3 and 10 centimetres of radar echo intensities from precipitation,' *Nat. Res. Coun. Canada, Rep.*, Ottawa, No. 2155.
Hooper, J. E. N. and Kippax, A. A.	1950	' Radar echoes from meteorological precipitation,' *Proc. Inst. Elect. Engrs.*, **97**, I, p. 89.
Hunter, I. M.	1954	' Polarization of radar echoes from meteorological precipitation,' *Nature*, **173**, p. 165.
Jones, D. M. A. and Dean, L. A.	1953	' Some observations from photographs of falling raindrops,' *Proc. Conf. Radio Met. Univ. Texas*, VIII-2.
Kerr, D. E., Ed.	1951	*Propagation of short radio waves*, M.I.T. Radiation Laboratory Series, **13**, New York (McGraw-Hill).
Labrum, N. R.	1952a	' Some experiments on centimetre wavelength scattering by small obstacles,' *J. Appl. Phys.*, **23**, p. 1320.
	1952b	' The scattering of radio waves by meteorological particles,' *J. Appl. Phys.*, **23**, p. 1324.
Lamb, J.	1946	' Measurements of the dielectric properties of ice,' *Trans. Faraday Soc.*, **42**A, p. 238.
Lamb, J. and Turney, A.	1949	' The dielectric properties of ice at 1·25 cm wavelength,' *Proc. Phys. Soc. Lond.*, B **62**, p. 272.
Lamont, H. R. L.	1948	'Atmospheric absorption of millimetre waves,' *Proc. Phys. Soc. Lond.*, **61**, p. 562.
Lane, J. A. and Saxton, J. A.	1952	' Dielectric dispersion in pure polar liquids at very high radio frequencies,' *Proc. Roy. Soc.* A, **213**, p. 400.
Langille, R. C. and Thain, R. S.	1951	' Some quantitative measurements of three-centimetre radar echoes from falling snow,' *Canadian J. Phys.*, **29**, p. 482.
Langleben, M. P. and Gunn, K. L. S.	1952	' Scattering and absorption of microwaves by a melting ice sphere,' *Stormy Weather Res. Group, McGill Univ., Scient. Rep.*, No. MW-5.
Laws, J. O. and Parsons, D. A.	1943	' The relation of raindrop size to intensity,' *Trans. Amer. Geophys. Un.*, **24**, p. 452.
Lowan, A., Ed.	1949	*Tables of scattering functions for spherical particles*, National Bureau of Standards, Washington.
Magono, Choji	1954	' On the shape of water drops falling in stagnant air,' *J. Met.*, **11**, p. 77.
Marshall, J. S.	1953	' The effects of wind shear on falling rain,' *Proc. Conf. Radio Met., Univ. Texas*, VIII-1.
Marshall, J. S. and Gunn, K. L. S.	1952	' Measurement of snow parameters by radar,' *J. Met.*, **9**, p. 322.
Marshall, J. S. and Hitschfeld, W.	1953	' The interpretation of the fluctuating echo from randomly distributed scatterers,' *Canadian J. Phys.*, **31**, p. 962.
Marshall, J. S., Hitschfeld, W., and Gunn, K. L. S.	1954	'Advances in radar weather,' *Advances in geophysics*, **2**, Ed. H. E. Landsberg, New York (Academic Press).
Marshall, J. S., Langille, R. C. and Palmer, W. McK.	1947	' Measurement of rainfall by radar,' *J. Met.*, **4**, p. 186.
Marshall, J. S. and Palmer, W. McK.	1948	' The distribution of raindrops with size,' *Ibid.*, **5**, p. 165.
Mie, G.	1908	*Ann. Physik*, **25**, p. 377.
Mt. Washington Observatory	1951	*Quart. Progr. Rep.*, 23 October.
Mueller, G. E.	1946	' Propagation of 6 millimetre waves,' *Proc. Inst. Radio Engrs.*, **34**, p. 181P.
Plank, V. G., Atlas, D. and Paulsen, W. H.	1952	'A preliminary survey of cloud and precipitation detection at 1·25 cm,' *Proc. Third Radar Weather Conf., McGill Univ.*, B-13.
Rigby, E. C., Marshall, J. S. and Hitschfeld, W.	1954	' The development of the size-distribution of raindrops during fall,' *J. Met.* (in course of publication).
Robertson, S. D. and King, A. P.	1946	' The effect of rain upon the propagation of waves in the 1- and 3-cm regions,' *Proc. Inst. Radio Engrs.*, **34**, p. 178P.
Ryde, J. W. and Ryde, D.	1945	'Attenuation of centimetre and millimetre waves by rain, hail, fogs and clouds,' *G.E.C. Res. Lab., Rep.* London, No. 8670.

Ryde, J. W.	1946	' The attenuation and radar echoes produced at centimetre wavelengths by various meteorological phenomena,' *Meteorological factors in radio wave propagation*, Phys. Soc., London.
Saxton, J. A. and Lane, J. A.	1946	' The anomalous dispersion of water at very high frequencies,' *Ibid.*
Silver, S.	1949	*Antenna theory and design*, M.I.T. Radiation Laboratory Series, **12**, New York (McGraw-Hill).
Sinclair, D.	1947	' Light scattering by spherical particles,' *J. Opt. Soc. Amer.*, **37**, p. 475.
Stevenson, A. F.	1953a	' Solution of electromagnetic scattering problems as power series in the ratio (dimension of scatterer)/wavelength,' *J. Appl. Phys.*, **24**, p. 1134.
	1953b	' Electromagnetic scattering by an ellipsoid in the third approximation,' *Ibid.*, **24**, p. 1143.
Stratton, J. A.	1941	*Electromagnetic theory*, New York (McGraw-Hill).
Swingle, D. M.	1953	'A review of results of operational tests of radar cloud detection equipment,' *Proc. Conf. Radio Met., Univ. Texas*, X-4.
Twomey, S.	1953	' On the measurement of precipitation by radar,' *J. Met.*, **10**, p. 66.
Van Vleck, J. H.	1947a	'Absorption of microwaves by oxygen,' *Phys. Rev.*, **71**, p. 413.
	1947b	'Absorption of microwaves by uncondensed water vapour, *Ibid.*, **71**, p. 425.
Wexler, R.	1948	' Rain intensities by radar,' *J. Met.*, **5**, p. 171.